Circulation Reports
Circ Rep 2019; 1: 46–54
doi:10.1253/circrep.CR-18-0016

ORIGINAL ARTICLE
Arrhythmia/Electrophysiology

Atypical Fast-Slow Atrioventricular Nodal Reentrant Tachycardia Utilizing a Slow Pathway Extending to the Inferolateral Right Atrium

Yoshiaki Kaneko, MD; Tadashi Nakajima, MD; Akihiko Nogami, MD; Yasuya Inden, MD; Tetsuya Asakawa, MD; Itsuro Morishima, MD; Akira Mizukami, MD; Takashi Iizuka, MD; Shuntaro Tamura, MD; Chihiro Ota, MD; Yasunori Kanzaki, MD; Kazuya Nakagawa, MD; Makoto Suzuki, MD; Masahiko Kurabayashi, MD

Background: The existence of atypical fast-slow (F/S) atrioventricular (AV) nodal reentrant tachycardias (NRT) using slow pathway (SP) variants connected to the right atrial (RA) inferolateral (inf) free wall (FW) along the tricuspid annulus (TA), has been neither confirmed nor precisely characterized.

Methods and Results: We studied 7 patients (mean age, 48±16 years; 5 men) with F/S-AVNRT with long RP intervals and an earliest atrial activation at the RA inf-FW along the TA (inf-F/S-AVNRT). AV reentrant tachycardia was excluded on observation of the transition zone criteria in all 7 patients. Atrial tachycardia was excluded on the observation of a V-A-V activation sequence after the induction or entrainment of the tachycardia from the right ventricle in all. During the tachycardia, low-frequency, fractionated potentials (LP) preceding the local atrial electrogram were recorded near the site of the earliest atrial activation in 6 patients. Observations of conduction delay and block of the LP during ventricular entrainment or ablation of the tachycardia indicated that LP reflect retrograde activation via the inf-SP. Retrograde SP conduction was interrupted at the site of earliest atrial activation in 3 patients, and in the right posterior septum in 4 patients.

Conclusions: inf-F/S-AVNRT are distinct supraventricular tachycardia incorporating an SP variant connected to the RA inf-FW along the TA in the retrograde direction, which were eliminated by ablation.

Key Words: Ablation; Atrioventricular nodal reentrant tachycardia; Electrophysiologic study; Slow pathway; Tricuspid annulus

Slow pathway (SP) is the main component of the reentry circuit responsible for the development of atrioventricular (AV) nodal reentrant tachycardia (NRT) and it is generally a target site of ablation to cure this arrhythmia.[1] Typical SP originates from the compact AV node and extends posteriorly in the Koch's triangle,[2,3] while it is individually viable in length.[2–4] Although variants of SP extending along the mitral annulus have been reported,[5,6] there is no previous report regarding the typical SP extending to the right atrial (RA) free wall (FW).[1–4] Herein, we describe an atypical type of fast-slow (F/S) AVNRT incorporating variants of the SP that extend to the inferolateral (inf) RA as a retrograde limb of the reentry circuit.

Methods

Subjects and Definition of inf-type F/S-AVNRT

We prospectively identified 2 women and 5 men, mean age 48±16 years (range, 25–72 years) at 6 Japanese medical institutions, who had undergone successful ablation of F/S-AVNRT presenting with long RP intervals and the earliest site of atrial activation during the tachycardia in the inf-FW of the RA adjacent to the tricuspid annulus (TA). The inferoanterior area of the RAFW was defined as the area ranging between 6 and 8:30 o'clock in the left anterior oblique fluoroscopic view. We diagnosed and named this unique AVNRT as inf-type F/S-AVNRT (inf-F/S-AVNRT) that utilized a fast pathway (FP) in the

Received November 27, 2018; revised manuscript received December 4, 2018; accepted December 6, 2018; J-STAGE Advance Publication released online January 10, 2019 Time for primary review: 1 day

Department of Cardiovascular Medicine, Gunma University Graduate School of Medicine, Maebashi (Y. Kaneko, T.N., T.I., S.T., M.K.); Cardiovascular Division, School of Medicine, University of Tsukuba, Tsukuba (A.N., C.O.); Department of Cardiology, Nagoya University Graduate School of Medicine, Nagoya (Y.I., Y. Kanzaki); Department of Cardiology, Yamanashi Kosei Hospital, Yamanishi (T.A., K.N.); Department of Cardiology, Ogaki Municipal Hospital, Ogaki (I.M.); Department of Cardiology, Kameda Medical Center, Kamogawa (A.M.); and Department of Cardiology, Yokohama Minami Kyosai Hospital, Yokohama (M.S.), Japan

Mailing address: Yoshiaki Kaneko, MD, PhD, Department of Cardiovascular Medicine, Gunma University Graduate School of Medicine, 3-39-22 Showa-machi, Maebashi 371-8511, Japan. E-mail: kanekoy@gunma-u.ac.jp

ISSN-2434-0790

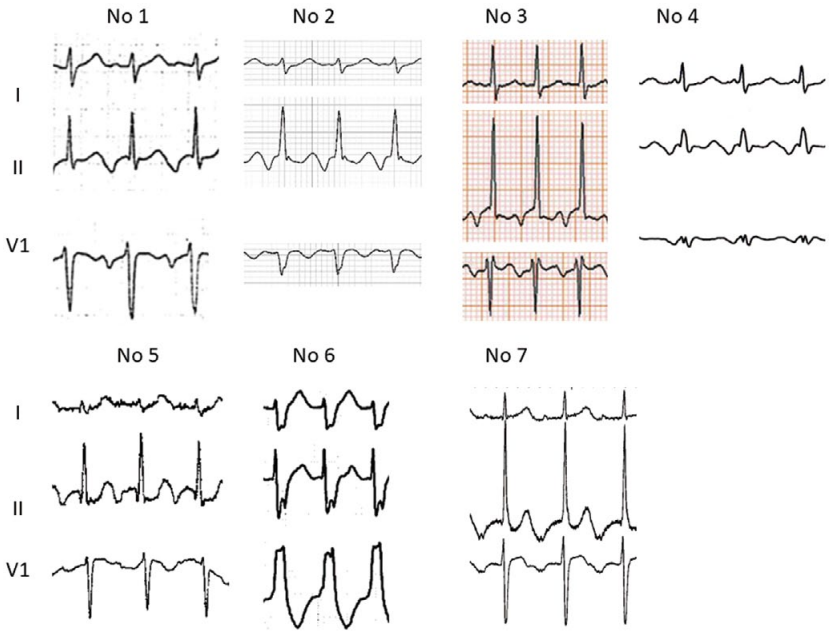

Figure 1. Surface electrocardiogram leads I, II and V1 recorded during tachycardia. The P waves were negative in lead II in patients 1–5 and 7, and isoelectric in patient 6. Note the long RP interval on all the recordings. QRS was wide in patient 6 due to ventricular aberrancy.

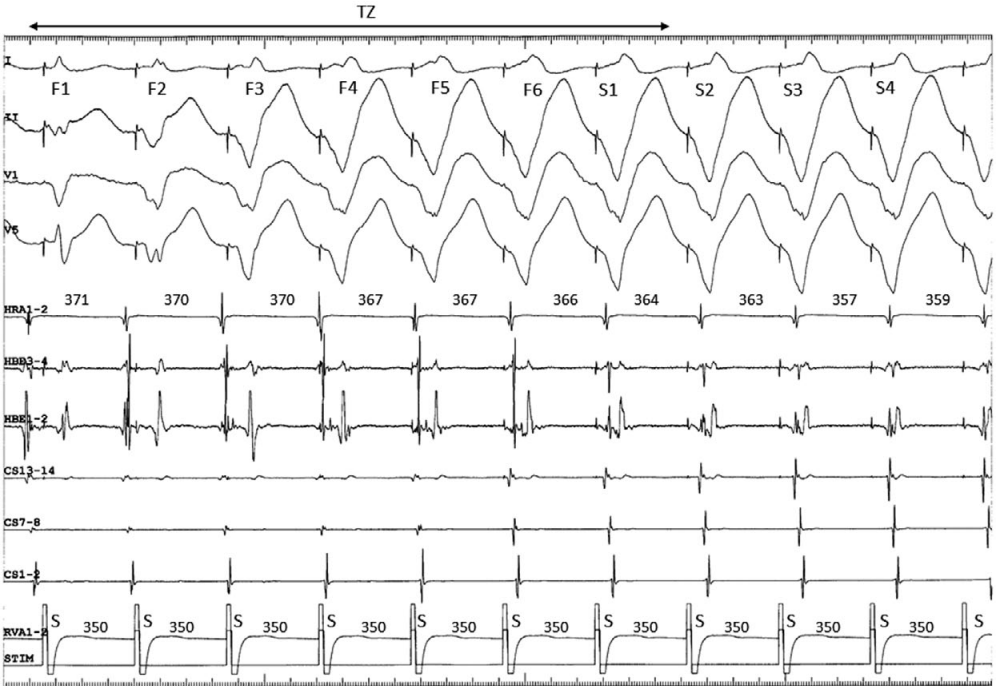

Figure 2. Intracardiac recordings showing the transition zone (TZ) criteria in patient 7. During isoproterenol infusion, the tachycardia accelerates and is sustained, without cycle length (CL) variations or spontaneous termination. Immediately after right ventricular (RV) overdrive pacing of the tachycardia at an S-S CL of 350 ms, there are 6 QRS complexes that demonstrate fusion (F1–F6) and thereafter the QRS morphology becomes stable (S1–S4). During the TZ (bidirectional arrow), the lack of perturbation of the atrial cycles and the lack of the increasing spike-atrial intervals are inconsistent with a diagnosis of atrioventricular reentrant tachycardia, and are consistent with a diagnosis of atrioventricular nodal reentrant tachycardias. The numbers between atrial electrograms at the high right atrium (HRA) and between the pacing stimuli at the RVA are CL in ms. I, II and V1, surface electrocardiogram; HRA1-2, distal HRA; HBE1-2 and 3-4, distal to proximal His bundle region; CS13-14 to 1-2, proximal-distal coronary sinus recording. Other data of this patient are shown in Figures 5,6.

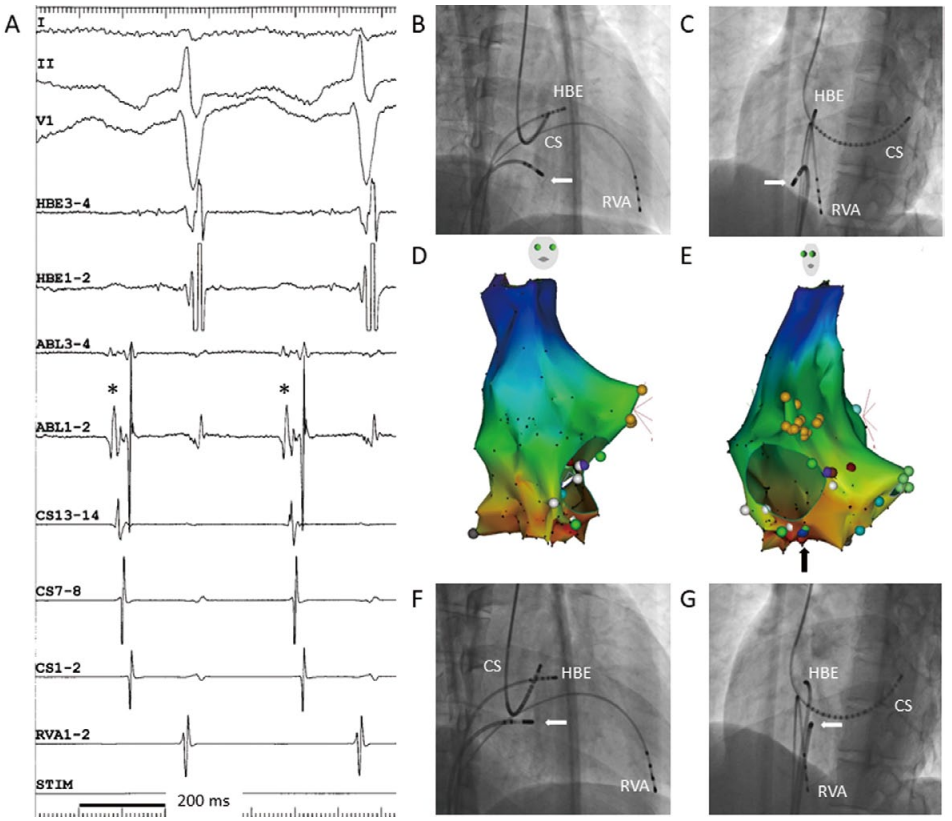

Figure 3. (**A**) Intracardiac recordings during tachycardia before successful radiofrequency delivery; (**B**,**C**,**F**,**G**) fluoroscopy of the position of the catheters, showing (**B**,**C**) the site of earliest atrial activation during the tachycardia (white arrows), and (**F**,**G**) the site of successful ablation (white arrows); (**D**,**E**) CARTO activation maps of the right atrium (RA) during the tachycardia in the right and left anterior oblique (LAO) views in patient 1. (**A**) Low-frequency potentials (asterisks) preceding the local atrial electrograms are recorded at the tip of ablation catheter (ABL1-2) located near the site of successful ablation. The low-frequency potentials also precede the earliest atrial activation, consistent with retrograde activation over the inferolateral slow pathway. (**D**,**E**) The distance between the site of earliest atrial activation registered at 7 o'clock in the LAO projection (blue tag marked by black arrow) and the site of successful ablation (purple tags) measured 21.2 mm, and that between the successful site and the nearest electrogram of His bundle (yellow tags) measured 17.6 mm. CS, coronary sinus; HBE, His bundle electrogram; RVA, right ventricular apex.

anterograde direction and utilized a variant of SP originating from the compact AV node and extending to the inf RA in the retrograde direction (inf-SP). This study complied with the guidelines of the Declaration of Helsinki and was approved by the institutional review board of Gunma University Hospital. Written informed consent to participate in this study was obtained from all patients.

Diagnosis of AVNRT

Electrophysiologic study were performed as described previously.[4,7]

First, orthodromic AV reentrant tachycardia (RT) utilizing a slowly conducting AV accessory pathway (AP) in the retrograde direction was excluded when at least one of the following criteria were met: (1) development of 2nd degree AV block during ongoing tachycardia;[8] (2) AV nodal response during parahisian pacing maneuver;[9–11] (3) response of AVNRT during differential ventricular entrainment pacing evidenced by a shorter stimulus-atrial electrogram (EGM) during entrainment pacing from the right ventricular (RV) apex than from the RV base (differential ventricular entrainment pacing);[12] (4) response of AVNRT during the transition zone characterized by progressive QRS fusion immediately after RV burst pacing of the tachycardia, evidenced by lack of perturbation of atrial cycles or lack of increasing spike-atrial interval (transition zone criteria);[13,14] (5) successful elimination or modification of the SP >2 cm away from the earliest site of atrial activation during the tachycardia; and (6) in the presence of successful ventricular entrainment, AVRT utilizing a concealed nodo-fascicular or nodo-ventricular AP in the retrograde direction was excluded by the absence of reset or termination of the tachycardia by premature ventricular stimulation during His bundle (HB) refractoriness.[15] The 5th criterion is based on the evidence that AP with slowly conducting properties including concealed atriofascicular fiber can always be ablated at the earliest site of atrial activation during retrograde conduction via the AP, and there is no report regarding obliquely coursing AP along the TA.[16–20] Second, atrial tachycardia (AT) was excluded if one or both of the following criteria were met: (1) termination of the tachycardia by ventricular pacing without atrial capture, followed or not by an orthodromic capture of the atria by ventricular pacing of the tachycardia,

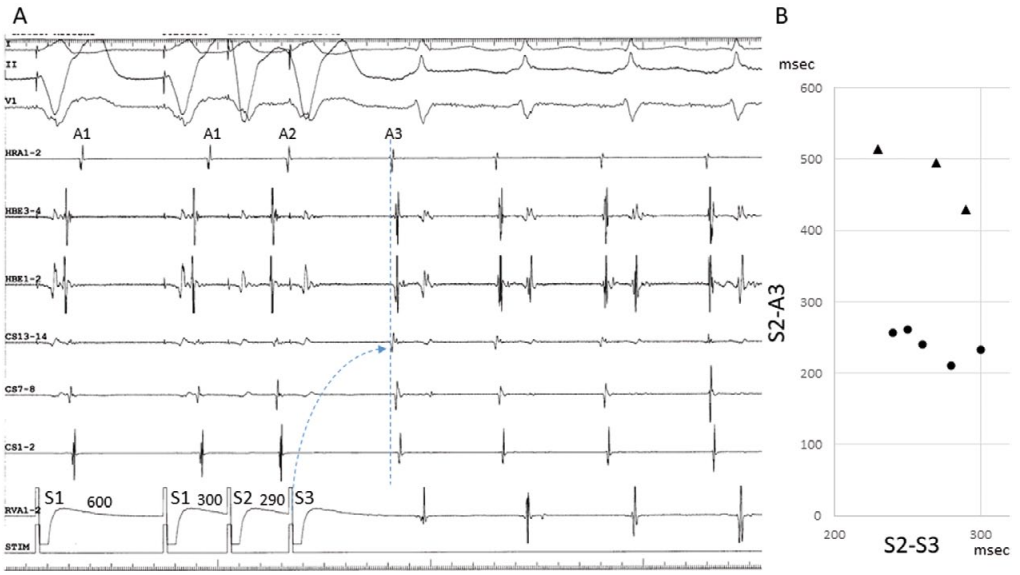

Figure 4. (**A**) Intracardiac recordings of an induction of the tachycardia with double extrastimulation from the right ventricular apex (RVA) and ventriculoatrial (VA) conduction curve in patient 7. After the first and second RVA stimulation at an S1–S1 cycle length of 600 ms, retrograde conduction over the fast pathway (FP; A1) is visible with the earliest site of atrial activation occurring in the His bundle (HB) region. After the S2 with an S1–S2 coupling interval of 300 ms, retrograde conduction over the FP (A2) also occurs, along with a conduction delay in the VA interval. When the S3 at an S2–S3 coupling interval of 290 ms causes a marked increase in the VA interval, retrograde conduction over the variant of slow pathway (SP) appears (A3; dotted arrow), followed by initiation of tachycardia. The earliest atrial activation on the A3 occurs simultaneously in the high right atrium (HRA) and the proximal coronary sinus (CS), identical to that during the tachycardia. Although not shown, single extrastimulation from the RVA did not induce the tachycardia, further indicating that the A3 is caused not by the A2, but by the S3, thus representing a V-A-V activation sequence that excludes the diagnosis of AT. Other abbreviations as in Figure 2. (**B**) When a retrograde conduction via the FP (●) is blocked, a retrograde conduction via the SP (▲) reproducibly occurs and is prolonged in the conduction time according to a decrease in the S2–S3 interval, consistent with frequency-dependent, decremental properties of the SP. Other data of this patient are shown in Figures 2,5.

manifesting as a >10-ms prolongation of the atrial cycle length (CL); or (2) a V-A-V activation sequence after ventricular induction/re-initiation of the tachycardia resulting from retrograde conduction over the variant of SP, followed by anterograde conduction over the FP.[21] Ventricular overdrive pacing during tachycardia was performed (1) during isoproterenol infusion to prevent spontaneous terminations of the tachycardia as well as fluctuations in the atrial CL during the tachycardia; and (2) at a pacing CL 10–30 ms shorter than the tachycardia, with a first stimulus synchronized to the ventricular EGM, and a delay 10 ms shorter than the tachycardia CL. Finally, the diagnosis of AVNRT was made on the exclusion of AVRT and AT.

Retrograde conduction over the variant of SP to the site of earliest atrial activation during tachycardia was strongly suspected when retrograde atrial activation after ventricular induction/entrainment with an initial V-A-V activation sequence was identical to that during tachycardia in patients with confirmed F/S-AVNRT.

Finally, the diagnosis of AVNRT was confirmed by elimination of the tachycardia after ablation of the SP variant.

Catheter Ablation

Before ablation, activation mapping of the RA was performed during ongoing tachycardia to determine the earliest site of activation, using the 3-D mapping systems in 6 patients or ablation catheter in the remaining patient. To ablate an inf-SP, we used the combined anatomical and EGM-guided method used for ablation of typical SP,[4] or targeted the site of earliest atrial activation during ongoing tachycardia. Radiofrequency (RF) energy was delivered at a power of 30 W with the temperature limited to 50°C regardless of the site of delivery, using a 7-F, 4-mm tip, non-irrigated ablation catheter. The recommended duration per delivery was a maximum of 40s. Ablation was successful when the tachycardia was non-inducible by programmed stimulation, before and during the infusion of isoproterenol.

Electrocardiography

We used surface 12-lead electrocardiograms (ECG) of the spontaneous or inducible tachycardia to determine the polarity of P waves that were not fused with the previous T wave or QRS complex. The P wave was visually assigned a positive, negative, biphasic (+/− or −/+) or isoelectric polarity.

Follow-up

The patients were followed 2– weeks after the ablation procedure, and at 6-month intervals thereafter. Procedure success was ascertained by the historical exclusion of tachycardia recurrences. All measurements are reported as mean ± SD.

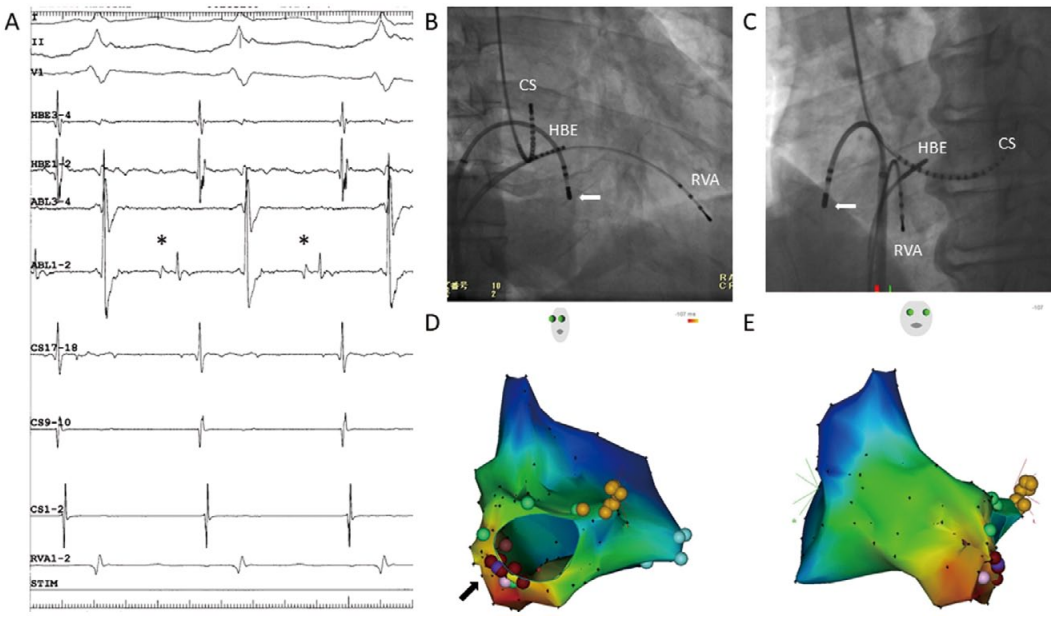

Figure 5. (**A**) Intracardiac recordings during tachycardia before successful radiofrequency energy delivery; (**B**,**C**) fluoroscopy of the position of the catheters, showing site of successful ablation (white arrows); (**D**,**E**) CARTO activation maps of the RA during the tachycardia in the right and LAO views in patient 7. (**A**) Low-frequency potentials (asterisks), consistent with retrograde activation over the inferolateral slow pathway, precede the atrial electrograms at the tip of ablation catheter (ABL1-2) located near the site of successful ablation (**D**,**E**, brown tags). (**B**–**E**) Earliest site of atrial activation during the tachycardia and the site of successful ablation are located at 8 o'clock in the LAO projection (**B**,**C**, white arrows; **D**,**E**, purple tags marked by black arrows). Other data of this patient are shown in Figures 2,4. Abbreviations as in Figure 3.

Results

Patient Characteristics

All patients were free from structural heart disease and all reported having palpitations. The episodes were paroxysmal and interrupted by prolonged periods of normal sinus rhythm. One patient had been unsuccessfully treated with verapamil.

Surface ECG

All 12-lead ECG recorded during spontaneous tachycardias indicated the presence of long RP intervals (**Figure 1**). The P-wave polarity in lead II was negative in 6 and isoelectric in 1 patient during the tachycardia.

Electrophysiological Diagnosis of AVNRT

Ventricular pre-excitation during sinus rhythm was not observed in any of the patient. Anterograde SP conduction, apparent as a sudden increase in the atrio-His interval, was observed in 3 patients. Retrograde conduction over the FP was observed in 6 patients.

AVRT was excluded on transition zone criteria in all 7 patients (**Figure 2**); on AV nodal response during parahisian pacing in patient 2; and on differential ventricular entrainment pacing in patient 1; and in patients 3 and 6, by the development of 2nd degree AV block during ongoing tachycardia. In 4 patients including the remaining 2 patients (patients 4 and 5), the SP was successfully ablated in the posterior septum, >3 cm away from the site of earliest atrial activation during tachycardia, excluding the diagnosis of AVRT (**Figure 3**). AT was excluded on observation of a V-A-V activation sequence after the induction (**Figure 4**) or entrainment of the tachycardia from the RV in all 7 patients.

The site of earliest atrial activation during tachycardia was at 8:00 o'clock in patient 7 (**Figure 5**), 7:00 o'clock in patients 1 (**Figure 3**) and 6, 6:30 o'clock in patients 4 and 5, and at 6:00 o'clock in patients 2 and 3 (**Table 1**). Retrograde conduction over the inf-SP was consistently reproducible during ventricular pacing in all patients (**Table 1**).

Catheter Ablation

Initially, we used the standard approach for the ablation of a typical SP in patient 1, and targeted the site of earliest activation during tachycardia in the remaining 6 patients. In patient 1, the ablation was successful in the posterior septum (**Figure 3**). In patients 3, 5 and 7, delivery of RF energy to the site of earliest activation terminated the tachycardia after a mean of 1.8±0.6 s (**Table 2**), whereas in patients 2, 4 and 6, the delivery of RF energy to the site of earliest activation was ineffective or only transiently effective, until we successfully used the standard approach. During the tachycardia, low-frequency, fractionated potentials (LP) preceding the atrial EGM were recorded near the site of the earliest atrial activation in 6 patients (**Table 2**; **Figures 3A**,**5A**,**6**). Interestingly, in patient 5, the LP represented conduction delay and block during ventricular entrainment (**Figure 6A**), and retrograde conduction block between the LP and the local atrial EGM developed during ablation of the SP, followed by the termination of the tachycardia (**Figure 6B**).[22] In all 7 patients, ectopic atrial complexes developed during RF energy delivery

Table 1. Electrophysiological Characteristics of SP and AVNRT Variants

Patient no.	Age (years)/ sex	SP						AVNRT									
		Pacing mode	ISO	Min S-A (ms)	R/G ERP v-SP (ms)	Min VP (ms)	DP	Induction mode	ISO	TCL (ms)	AH (ms)	HA (ms)	AVB	TZC	V-A-V (I)/V-A-V (E)/DAR	Term w/o A	SEA (o'clock)
1	25/M	VOP, PVS	+	374	440	380	+	PAS	+	337	62	275	–	+	+/+/–	–	7
2	39/M	VOP, PVS	–	430	220	400	+	AOP, PAS, VOP, PVS	–	438	73	365	–	+	+/+/–	–	6
3	62/F	PVS	–	321	270	ND	ND	PAS	–	402	186	216	+	+	–/+/–	–	6
4	72/M	VOP, PVS	–	259	ND	ND	ND	PAS	–	444	94	350	–	+	–/+/+	–	6:30
5	38/F	VOP, PVS, sPVS	–	524	580	900	+	PAS, VOP	+	365	110	255	–	+	+/+/–	+	6:30
6	38/M	VOP	+	450	NM	NM	ND	PAS	+	313	63	250	+	+	–/+/–	–	7
7	61/M	PVS	–	442	200	NM	+	VOP, PVS, PAS, AOS	–	492	51	441	–	+	+/+/+	–	8
Mean ± SD				400± 82	342± 146	560± 241				399± 59	91± 43	307± 74					

AH, atrio-His interval; AOP, atrial overdrive pacing; AOS, atrial overdrive pacing; ATP, lowest dose of adenosine triphosphate terminating the tachycardia; AVB, atrioventricular block during ongoing tachycardia; AVNRT, atrioventricular nodal reentrant tachycardia; DP, decremental properties; HA, His-atrial interval; ISO, isoproterenol infusion; Min S-A, shortest stimulus-atrial electrogram interval; Min VP, shortest ventricular pacing cycle length associated with 1:1 VA conduction; ND, not determined; NM, not measured; PAS, premature atrial stimulation; PVS, premature ventricular stimulation; R/G ERP v-SP, retrograde effective refractory period of variant of slow pathway; SEA, site of earliest atrial activation; SP, slow pathway; sPVS, premature ventricular stimulation after simultaneous atrial and ventricular pacing; TCL, tachycardia cycle length; Term w/o A, termination of tachycardia by ventricular pacing without atrial capture; TZC, transition zone criteria; V-A-V (I), V-A-V activation sequence after ventricular induction pacing; V-A-V (E), V-A-V activation sequence after ventricular entrainment; VOP, ventricular overdrive pacing.

Table 2. Ablation of Slow Pathway and Follow-up Observations

Patient no.	Successful ablation site			EGM at the site of the earliest activation					RF energy		After ablation			
	o'clock	H-distance (mm)	T-distance (mm)	A-P (ms)	A (mV)	V (mV)	A/V	PreP	EJC	Duration (s)†	Outcome	R/G v-SP	Follow-up (months)	Rec
1	4	17.6	8.7	NM	0.13	0.54	0.24	+	+	NM	Tachycardia non-inducible	–	63	–
2	4	NM	NM	NM	0.26	1.80	0.14	–	+	NM	Tachycardia non-inducible	–	108	–
3	6	51	NM	–10	0.05	0.22	0.22	+	–	2.6	Tachycardia non-inducible	–	6	–
4	5	NM	NM	–51	0.3	0.58	0.52	+	+	2.9	Tachycardia non-inducible	+	10	–
5	6:30	19	NM	–22	0.49	1.3	0.38	+	+	1.7	Tachycardia non-inducible	–	18	–
6	5	NM	NM	–48	0.33	1.04	0.32	+	+	7.2	Tachycardia non-inducible	–	5	–
7	8	29.7	4.5	–36	0.35	0.69	0.51	+	+	1.2	Tachycardia non-inducible	–	1	–
Mean ± SD		29± 13	6.6± 2.1	–33± 16	0.27± 0.13	0.88± 0.50	0.33± 0.13			3.1± 2.1			31± 34	

†Time to tachycardia termination. A and V, amplitudes of atrial and ventricular EGM; A-P, timing of local atrial EGM relative to the onset of P wave; A/V, atrial/ventricular EGM ratio; EGM, electrogram; EJC, ectopic junctional complex; H-distance, distance between ablation site and His-bundle; NM, not measured; PreP; potential preceding atrial EGM; Rec, recurrence; RF, radiofrequency; R/G v-SP, retrograde conduction over slow pathway variant; T-distance, distance between ablation site and tricuspid annulus.

(**Table 2**). In patients 6 and 7, subtle changes in the site of earliest atrial activation during tachycardia were observed immediately after the application of RF energy.

After ablation, neither AV block nor abnormal antegrade conduction over the FP was observed in any patient, and AVNRT was no longer inducible by atrial or ventricular stimulation before or during the infusion of isoproterenol (**Table 2**). During follow-up, no patient complained of recurrences of tachycardia (**Table 2**).

Discussion

Electrophysiological Characteristics of inf-F/S-AVNRT

inf-F/S-AVNRT is characterized by the site of earliest

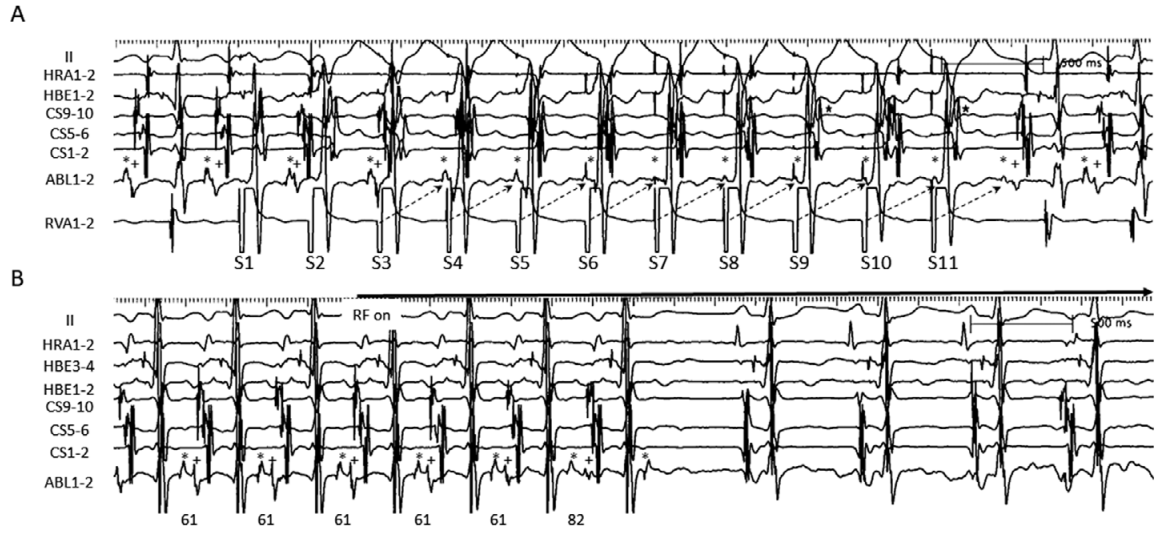

Figure 6. Intracardiac recordings of low-frequency potentials (LP) reflecting retrograde activation over the inferolateral slow pathway (asterisks) during the (**A**) tachycardia and ventricular entrainment and (**B**) radiofrequency energy delivery in patient 5. (**A**) During tachycardia, the LP are recorded, followed by the local atrial electrogram (EGM; +) at the tip of ABL1-2. The S3 and the subsequent stimuli during ventricular entrainment with a cycle length of 340 ms capture the LP with a slight conduction delay of a spike-LP interval (dotted arrows), followed by conduction block between the LP and the atrial EGM with 2:1 ratio developing after the S8 and S10, respectively (★). (**B**) Immediately after a slight prolongation of the interval between the LP and the atrial EGM (displayed by numbers in ms) was observed between the 2nd and 3rd tachycardia cycle during RF energy delivery, the tachycardia terminated with an end of the LP. Other abbreviations as in Figure 2. Modified from Nakagawa K, et al[22] with permission of the publisher. Copyright © 2018, the Japanese Society of Clinical Cardiac Electrophysiology.

atrial activation in the inf FW of the RA adjacent to the TA. This eccentric atrial activation during tachycardia with long RP intervals has been considered a sign in support of the diagnosis of AT[23–25] or of AVRT incorporating slowly conducting AV AP[15–18] or concealed nodoventricular fiber.[19] We believe that the electrophysiological criteria applied by us successfully excluded the diagnosis of AT and of AVRT.

This F/S-AVNRT has not been reported previously,[26–28] and is a new variety of F/S-AVNRT, despite its successful ablation in the standard posteroseptal region in some instances. Eccentric atrial activation during tachycardia originating away from the septum has been considered a sign in support of the diagnosis of AT.[29] The present observations suggest, however, that this criterion should be reconsidered. Diagnosis of this type of F/S-AVNRT, however, requires meticulous mapping of the site of earliest atrial activation during tachycardia, which, if not performed, might not be recognized by the operator. Thus, patients with inf-F/S-AVNRT may be included with patients presenting with F/S-AVNRT successfully ablated by standard techniques, used for the treatment of typical SP.

Electrophysiological confirmation of F/S-AVNRT with a site of earliest atrial activation in the RAFW near the TA strongly supports the presence of a variant of SP extending to that earliest site. Interestingly, in most patients (75%) with this F/S-AVNRT, the LP were detected near the site of the earliest atrial activation during the tachycardia (**Table 2**; **Figures 3A**,**5A**,**6**). Although it is well-known that multiple potentials, so-called Jackman potentials[30] or Haissaguarre potentials,[31] can be detected during sinus rhythm in Koch's triangle, detection of the LP during the ongoing F/S-AVNRT outside Koch's triangle has not been described previously. Moreover, it is noteworthy that (although observed in only 1 patient), conduction delay and block of the LP during ventricular entrainment (**Figure 6A**), and development of retrograde conduction block between the LP and the local atrial EGM during ablation of the SP, followed by the termination of the tachycardia (**Figure 6B**) was observed. This indicates that LP reflect retrograde activation over the inf-SP. Therefore, it is possible that detection of the LP helps the physician localize the SP as the putative target of ablation.

The inf-SP were successfully ablated with the standard techniques used for typical SP or at the site of earliest atrial activation. An accelerated junctional rhythm during ablation was frequently observed during RF energy delivery near the earliest site of atrial activation in the RAFW, as in the case of a typical SP, and might be an indicator of the heating effect on AV nodal transitional cells constituting these variants of SP.[32] The successful ablation at a traditional ablation site confirmed the presence of an SP that traverses Koch's triangle. In some patients, however, the tachycardia was refractory to cure, requiring multiple RF energy applications, accompanied by shifts of the site of earliest atrial activation during the tachycardia. These phenomena may suggest structural characteristics of inf-SP such as a relatively broad, incompletely dissociated tissue with multiple connections to atrial muscle.

Putative Role of AV Ring Tissue in the Genesis of inf-SP

Although SP variants extending into the inf RAFW have not been confirmed histologically,[2] several studies have helped clarify the genesis of the inf-SP. Anderson and

Taylor noted specialized atrial tissue surrounding the TA, distinct from other atrial myocytes in humans,[33] McGuire et al described cells with nodal-like characteristics around the entire TA, including their cellular electrophysiology, response to adenosine, and lack of connexin43, and suggested that these cells may be the substrate of the slow "AV nodal" pathway.[34] Furthermore, several studies have suggested that AV rings of nodal-like myocytes surround the TA,[35–38] and are anatomically continuous with inferior extensions of the AV node.[38–40] This continuity between the AV node and AV ring tissue may be attributable to the embryological development of the AV ring and AV node from an identical origin, the so-called embryonic AV canal.[38–40] The anatomic connection of the compact AV node to the inferior AV ring tissue in humans, forming the SP, however, remains to be clarified. Nevertheless, we hypothesize, given the present electrophysiological findings, that a primitive form of inf-SP is created by the AV ring at least electrophysiologically connected to inferior extensions of the AV node.

Study Limitations

There were some limitations in the present study. First, this retrospective study, which was limited to cases of successful ablation, was small. Therefore, the overall safety and efficacy of this therapy and the optimal selection of the ablation site remain to be firmly established. A larger, prospective study is needed to clarify these points. Second, the type and number of poles of electrode catheters used were not uniform in this study. The bipole electrodes located in the proximal coronary sinus were confirmed on fluoroscopy, however, at each institute.

Conclusions

inf-F/S-AVNRT are distinct supraventricular tachycardias, which use a variant of SP located along the TA as the retrograde limb, and which can be eliminated with RF ablation.

Acknowledgment

Y. Kaneko was supported by a Grant-in-Aid for Scientific Research (No. 16K09418) from the Japanese Society for the Promotion of Science.

Disclosures

The authors declare no conflicts of interest.

References

1. Lockwood D, Nakagawa H, Jackman WM. Electrophysiologic characteristics of atrioventricular nodal reentrant tachycardia: Implications for reentrant circuits. *In*: Zipes DP, Jalife J, editors. Cardiac electrophysiology: From cell to bedside, 7th edn. Philadelphia: WB Saunders, 2018; 746–767.
2. Inoue S, Becker AE. Posterior extensions of the human compact atrioventricular node: A neglected anatomic feature of potential clinical significance. *Circulation* 1998; **97:** 188–193.
3. McGuire MA, Bourke JP, Robotin MC, Johnson DC, Meldrum-Hanna W, Nunn GR, et al. High resolution mapping of Koch's triangle using sixty electrodes in humans with atrioventricular junctional (AV nodal) reentrant tachycardia. *Circulation* 1993; **88**(5 Pt 1)**:** 2315–2328.
4. Irie T, Kaneko Y, Nakajima T, Ota M, Iijima T, Tamura M, et al. Electroanatomically estimated length of slow pathway in atrioventricular nodal reentrant tachycardia. *Heart Vessels* 2014; **29:** 817–824.
5. Katritsis DG, John RM, Latchamsetty R, Muthalaly RG, Zografos T, Katritsis GD, et al. Left septal slow pathway ablation for atrioventricular nodal reentrant tachycardia. *Circ Arrhythm Electrophysiol* 2018; **11:** e005907.
6. Stavrakis S, Jackman WM, Lockwood D, Nakagawa H, Beckman K, Elkholey K, et al. Slow/fast atrioventricular nodal reentrant tachycardia using the inferolateral left atrial slow pathway. *Circ Arrhythm Electrophysiol* 2018; **11:** e006631.
7. Kaneko Y, Naito S, Okishige K, Morishima I, Tobiume T, Nakajima T, et al. Atypical fast-slow atrioventricular nodal reentrant tachycardia incorporating a "superior" slow pathway: A distinct supraventricular tachyarrhythmia. *Circulation* 2016; **133:** 114–123.
8. Yeh SJ, Yamamoto T, Lin FC, Wu D. Atrioventricular block in the atypical form of junctional reciprocating tachycardia: Evidence supporting the atrioventricular node as the site of reentry. *J Am Coll Cardiol* 1990; **15:** 385–392.
9. Hirao K, Otomo K, Wang X, Beckman KJ, McClelland JH, Widman L, et al. Para-Hisian pacing. A new method for differentiating retrograde conduction over an accessory AV pathway from conduction over the AV node. *Circulation* 1996; **94:** 1027–1035.
10. Nakagawa H, Jackman WM. Para-Hisian pacing: Useful clinical technique to differentiate retrograde conduction between accessory atrioventricular pathways and atrioventricular nodal pathways. *Heart Rhythm* 2005; **2:** 667–672.
11. Sheldon SH, Li HK, Asirvatham SJ, McLeod CJ. Parahisian pacing: Technique, utility, and pitfalls. *J Interv Card Electrophysiol* 2014; **40:** 105–116.
12. Bennett MT, Leong-Sit P, Gula LJ, Skanes AC, Yee R, Krahn AD, et al. Entrainment for distinguishing atypical atrioventricular node reentrant tachycardia from atrioventricular reentrant tachycardia over septal accessory pathways with long-RP [corrected] tachycardia. *Circ Arrhythm Electrophysiol* 2011; **4:** 506–509.
13. AlMahameed ST, Buxton AE, Michaud GF. New criteria during right ventricular pacing to determine the mechanism of supraventricular tachycardia. *Circ Arrhythm Electrophysiol* 2010; **3:** 578–584.
14. Dandamudi G, Mokabberi R, Assal C, Das MK, Oren J, Storm R, et al. A novel approach to differentiating orthodromic reciprocating tachycardia from atrioventricular nodal reentrant tachycardia. *Heart Rhythm* 2010; **7:** 1326–1329.
15. Ho RT, Frisch DR, Pavri BB, Levi SA, Greenspon AJ. Electrophysiological features differentiating the atypical atrioventricular node-dependent long RP supraventricular tachycardias. *Circ Arrhythm Electrophysiol* 2013; **6:** 597–605.
16. Gaita F, Haissaguerre M, Giustetto C, Fischer B, Riccardi R, Richiardi E, et al. Catheter ablation of permanent junctional reciprocating tachycardia with radiofrequency current. *J Am Coll Cardiol* 1995; **25:** 648–654.
17. Ticho BS, Saul JP, Hulse JE, De W, Lulu J, Walsh EP. Variable location of accessory pathways associated with the permanent form of junctional reciprocating tachycardia and confirmation with radiofrequency ablation. *Am J Cardiol* 1992; **70:** 1559–1564.
18. Meiltz A, Weber R, Halimi F, Defaye P, Boveda S, Tavernier R, et al. Permanent form of junctional reciprocating tachycardia in adults: Peculiar features and results of radiofrequency catheter ablation. *Europace* 2006; **8:** 21–28.
19. Kang KT, Potts JE, Radbill AE, La Page MJ, Papagiannis J, Garnreiter JM, et al. Permanent junctional reciprocating tachycardia in children: A multicenter experience. *Heart Rhythm* 2014; **11:** 1426–1432.
20. Dubin AM, Desai K, Van Hare GF. Reentrant tachycardia using two discrete atrioventricular nodes and a concealed atriofascicular pathway. *Pediatr Cardiol* 2001; **22:** 400–402.
21. Knight BP, Zivin A, Souza J, Flemming M, Pelosi F, Goyal R, et al. A technique for the rapid diagnosis of atrial tachycardia in the electrophysiology laboratory. *J Am Coll Cardiol* 1999; **33:** 775–781.
22. Nakagawa K, Asakawa T, Yamada R, Sugawara C, Mochida T, Matsumura K, et al. A case of atypical fast-slow atrioventricular nodal reentrant tachycardia: Electrophysiological characteristics and catheter ablation. *J Jpn Soc Clin Card Electrophysiol* 2018; **41:** 259–266.
23. Yamabe H, Tanaka Y, Okumura K, Morikami Y, Kimura Y, Hokamura Y, et al. Electrophysiologic characteristics of verapamil-sensitive atrial tachycardia originating from the atrioventricular annulus. *Am J Cardiol* 2005; **95:** 1425–1430.
24. Kistler PM, Roberts-Thomson KC, Haqqani HM, Fynn SP, Singarayar S, Vohra JK, et al. P-wave morphology in focal atrial tachycardia: Development of an algorithm to predict the

anatomic site of origin. *J Am Coll Cardiol* 2006; **48:** 1010–1017.
25. Yamabe H, Okumura K, Koyama J, Kanazawa H, Hoshiyama T, Ogawa H. Demonstration of anatomic reentrant circuit in verapamil-sensitive atrial tachycardia originating from the atrioventricular annulus other than the vicinity of the atrioventricular node. *Am J Cardiol* 2014; **113:** 1822–1828.
26. Yu WC, Chen SA, Tai CT, Lee SH, Chiang CE, Wen ZC, et al. Electrophysiologic characteristics and radiofrequency catheter ablation of fast-slow form atrioventricular nodal reentrant tachycardia. *Am J Cardiol* 1997; **79:** 683–686.
27. Lee KL, Chun HM, Liem LB, Lauer MR, Young C, Sung RJ. Multiple atrioventricular nodal pathways in humans: Electrophysiologic demonstration and characterization. *J Cardiovasc Electrophysiol* 1998; **9:** 129–140.
28. Yamabe H, Shimasaki Y, Honda O, Kimura Y, Hokamura Y. Demonstration of the exact anatomic tachycardia circuit in the fast-slow form of atrioventricular nodal reentrant tachycardia. *Circulation* 2001; **104:** 1268–1273.
29. Saoudi N, Cosío F, Waldo A, Chen SA, Iesaka Y, Lesh M, et al. A classification of atrial flutter and regular atrial tachycardia according to electrophysiological mechanisms and anatomical bases; a Statement from a Joint Expert Group from The Working Group of Arrhythmias of the European Society of Cardiology and the North American Society of Pacing and Electrophysiology. *Eur Heart J* 2001; **22:** 1162–1182.
30. Jackman WM, Beckman KJ, McClelland JH, Wang X, Friday KJ, Roman CA, et al. Treatment of supraventricular tachycardia due to atrioventricular nodal reentry by radiofrequency catheter ablation of slow-pathway conduction. *N Engl J Med* 1992; **327:** 313–318.
31. Haissaguerre M, Gaita F, Fischer B, Commenges D, Montserrat P, d'Ivernois C, et al. Elimination of atrioventricular nodal reentrant tachycardia using discrete slow potentials to guide application of radiofrequency energy. *Circulation* 1992; **85:** 2162–2175.
32. Boyle NG, Anselme F, Monahan K, Papageorgiou P, Zardini M, Zebede J, et al. Origin of junctional rhythm during radiofrequency ablation of atrioventricular nodal reentrant tachycardia in patients without structural heart disease. *Am J Cardiol* 1997; **80:** 575–580.
33. Anderson RH, Taylor IM. Development of atrioventricular specialized tissue in human heart. *Br Heart J* 1972; **34:** 1205–1214.
34. McGuire MA, de Bakker JM, Vermeulen JT, Moorman AF, Loh P, Thibault B, et al. Atrioventricular junctional tissue: Discrepancy between histological and electrophysiological characteristics. *Circulation* 1996; **94:** 571–577.
35. Anderson RH. The disposition and innervation of atrioventricular ring specialized tissue in rats and rabbits. *J Anat* 1972; **113**(Pt 2)**:** 197–211.
36. Yanni J, Boyett MR, Anderson RH, Dobrzynski H. The extent of the specialized atrioventricular ring tissues. *Heart Rhythm* 2009; **6:** 672–680.
37. Atkinson AJ, Logantha SJ, Hao G, Yanni J, Fedorenko O, Sinha A, et al. Functional, anatomical, and molecular investigation of the cardiac conduction system and arrhythmogenic atrioventricular ring tissue in the rat heart. *J Am Heart Assoc* 2013; **2:** e000246.
38. Aanhaanen WT, Mommersteeg MT, Norden J, Wakker V, de Gier-de Vries C, Anderson RH, et al. Developmental origin, growth, and three-dimensional architecture of the atrioventricular conduction axis of the mouse heart. *Circ Res* 2010; **107:** 728–736.
39. Sizarov A, Ya J, de Boer BA, Lamers WH, Christoffels VM, Moorman AF. Formation of the building plan of the human heart: Morphogenesis, growth, and differentiation. *Circulation* 2011; **123:** 1125–1135.
40. van Weerd JH, Christoffels VM. The formation and function of the cardiac conduction system. *Development* 2016; **143:** 197–210.